Computerized tool for identification and enhanced visualization of Macular Edema regions using OCT scans

Iago Otero[1,2], Plácido L. Vidal[1,2], Joaquim de Moura[1,2],
Jorge Novo[1,2] and Marcos Ortega[1,2] *

1 - Department of Computer Science, University of A Coruña, A Coruña (Spain)

2 - CITIC - Research Center of Information and Communication Technologies,
University of A Coruña, A Coruña (Spain)

Abstract.   We propose a novel methodology using Optical Coherence Tomography (OCT) images to detect the 3 clinically defined types of Macular Edema, which is among the main causes of blindness: Diffuse Retinal Thickening (DRT), Cystoid Macular Edema (CME) and Serous Retinal Detachment (SRD). To perform this detection, we sample the images and train models to create an intuitive color map that represents the 3 pathologies to facilitate the clinical evaluation. The proposed method was tested using a dataset composed by 96 OCT images. The system provided satisfactory results with accuracy values of 90.49%, 93.23% and 88.87% for the CME, SRD and DRT detections, respectively.

1   Introduction

Over 80% of all the vision impairment can be prevented or cured. Despite this, 253 million people live with vision impairment according to the World Health Organization [1]. Uncorrected refractive errors are currently the top cause of vision loss, followed by un-operated cataract and macular disorders, being Macular Edema (ME) one of the most relevant, characterized as intraretinal fluid accumulations in the macular region.

Currently, the control, diagnosis and monitoring of ME is performed through the analysis of Optical Coherence Tomography (OCT) images, an ophthalmological image modality that directly permits the measurement of the thickness of the retinal region and the analysis of the included layer tissue in a non-invasive way [2]. Based on this image modality, Otani *et al.* [3] defined a clinical classification of 3 different patterns of structural changes in which the disorder can appear. This definition was subsequently expanded by Panozzo *et al.* [4], being the international clinical classification of reference. The 3 types, defined by the authors, are the following: Diffuse Retinal Thickening (DRT), Cystoid Macular Edema (CME) and Serous Retinal Detachment (SRD). DRT is characterised
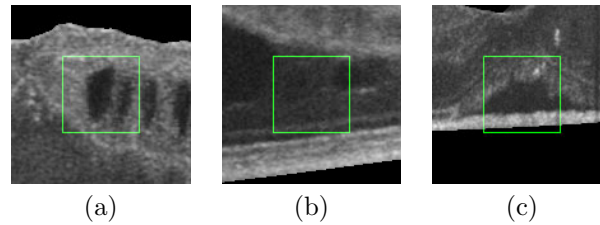

Fig. 1: Examples of ME regions. (a) CME, (b) DRT and (c) SRD.

by an increased retinal thickness with reduced intraretinal reflectivity, typically located in the inner retina. CMEs are defined as intraretinal cystoid spaces at the macular region with ovoid shapes and no reflectivity. SRD is known as a subretinal fluid accumulation above the hyper-reflective line of the pigmented epithelium. Figure 1 shows some representative examples of each ME type.

In recent years, some contributions have emerged related to this topic. These proposals partially analyse the pathology focusing mainly on the cystoid type, identifying the fluid presence in the intraretinal layers. These proposed methods are based, generally, in the use of image processing techniques combined, in some cases, with learning strategies. They are used for the initial detection of candidates and a posterior analysis based on morphological and/or intensity features to remove false positives (FPs). Following this strategy, as reference, Wilkins *et al.* [5] faced the CME identification by a combination of an initial thresholding followed by a FP reducing using a couple of rules to obtain the final results. Other strategy was followed by de Moura *et al.* [6] [7], analyzing windows of a given size to determine the presence of cystoid regions. A set of intensity or texture features is used to perform the analysis. Sidibé *et al.* [8] models the appearance of normal OCT images with a Gaussian Mixture Model (GMM) and, therefore, detect abnormal images as outliers. Similarly, Montuoro *et al.* [9] proposes a 3D method that segments the retinal layers and fluid regions to identify abnormal cases. Alsaih *et al.* [10] used machine learning techniques to classify normal and diabetic ME cases.

As said, most of the proposals faced partially the ME disease by the analysis of the cystoid fluid cases. The only approach that tackled the complete pathology with the identification of the 3 types is the work of Samagaio *et al.* [11]. In this work, specific strategies using image processing techniques were applied to localize the presence of each ME type. However, the majority of the proposals come with the same drawback: as explained, a posterior removal of FPs is needed in almost all the proposals. This can lead to mistakenly discarding true positive cases and even provoke confusion in the posterior morphological and intensity analysis. Also, sometimes, the boundary of the edemas may be largely diffuse, or appearing as nearby groups that harden enormously the segmentation process.

In this work, a novel method is proposed that addresses a regional identification of the 3 ME categories following the clinical classification of international reference in the ophthalmological field, building an intuitive color map that rep-

resents the simultaneous occurrence of each of them to help the ophthalmologists to achieve more accurate diagnoses and treatments.

2 Methodology

The method is divided in 4 main stages: region of interest delimitation, extraction of representative samples, feature selection and classification, and creation of a binary map for each model, being merged into 1 intuitive color map.

2.1 Retinal Layer Segmentation

The proposed system identifies the 2 limiting retinal layers: the Inner Limiting Membrane (ILM) and the Retinal Pigment Epithelium (RPE). To achieve this, a method based on the work of Chiu *et al.* [12] was employed. This method uses graph theory with intensity gradient information to find the retinal layers, representing each image as a graph of nodes. Dark-to-light and light-to-dark gradients are calculated in order to identify the ILM and RPE limits, respectively, given their contrast characteristics. These gradients are, then, used as weights in the search for the minimum weighted paths, performed by the Dijkstra's algorithm.

2.2 Feature measurement

An expanded set of 375 features [13] was used to identify the 3 different types of ME. This set includes intensity and texture-based features that help in the discrimination of the disease regions and the normal areas of the retina.

The intensity-based features are important because, typically, pathological areas present higher irregularities in their gray level distribution than the normal retinal tissue. For that purpose, we use mean, median, standard deviation, variance and other gray-level global distribution statistics. Also, texture-based features are relevant given they describe internal characteristics that help to differentiate the pathological tissue. We use eigenvalues, Gray-Level Intensity Histogram, Gray-Level Co-Occurrence Matrix, Histogram of Oriented Gradients, Gabor filters, Local Binary Patterns, LAWS filters, fractal dimension features and Gray-Level Run Length Image Statistics.

2.3 Feature Selection and Classification

A feature selection process was performed using Sequential Forward Selection (SFS) with inter-intra feature distance as criterion. Doing this, we are able to avoid redundant features and speed up the classification stage.

Three different models were trained and tested, one for each type of ME. The Linear Bayes Normal Classifier (LDC) and k-nearest neighbors (kNN) were used as representative classifiers that offered satisfactory results in similar approaches [6][7]. In the case of kNN, 3 empirically determined configurations were analyzed, using $k = [3,5,7]$. Additionally, a variant of the kNN method, Parzen, was used based on the satisfactory performance of the kNN classifier.

2.4 Map Generation

To create the color map, the entire region of interest is uniformly analyzed using samples of a given size and with an specific overlap among them. Each sample is, then, classified with the 3 trained models. Each one of them determines whether its type of ME is present in that sample. Then, for each ME type, a binary map is created. This is done by assigning the central point of each sample and its nearest pixels to the identified category.

Lastly, in order to produce a global intuitive map, the 3 binary maps are merged assigning each individual map to a primary color of each channel of the RGB model. This way, a positive detection of CME is represented in red, DRT in green whereas SRD in blue. Therefore, if multiple types of ME are detected in the same area, it will result in the secondary colors composed by the 2 or 3 corresponding channels of RGB, e.g., a multiple detection of CME and SRD would have red and blue channels activated, resulting in the magenta color.

3 Results and Discussion

The proposed methodology was validated using a dataset of 96 OCT retinal images centered in the macula and captured with a confocal scanning laser ophtalmoscope, a CIRRUS^{TM}HD-OCT-Carl Zeiss Meditec. The resolution of these images ranges from 924×616 to 1200×800. Images with different intensity and contrast properties are present in this set. No preprocessing stage was performed to the images, using, directly, the captured image characteristics.

This dataset was labeled by an expert clinician, identifying the 3 types of ME in each OCT image. Using this ground-truth as reference, training and testing sets were build for each category. In the case of CMEs, 527 pathological and 441 normal samples were used. For the DRT type, 236 and 323 were extracted, respectively. Finally, for the SRD case, 67 pathological and 217 normal samples were studied. The lower number of SRD samples is determined by the lower presence of this type, given it affects only to a reduced number of patients [3]. In these sets, the window size of each sample was established to 61×61, as a suitable previously determined size [6].

The individual performance of each system was measured by a 10-fold cross-validation with 50 repetitions using different training and testing sets, equally represented. Regarding the feature selection process, the predominant features were the Gabor filters, HOG and LBP, as they include a high potential of differentiation between the intraretinal fluid accumulation and the normal tissue. Also, the eigenvalues were specially valuable to discriminate the SRD case.

Table 1 shows the performance of the best configurations of feature sets and classifiers facing each type of ME, being 50 the maximum number of features. In the CME case, the best results were obtained with the LDC classifier using 42 features, which resulted in a satisfactory accuracy of 0.9049. On the other hand, the classifier with the best performance for the SRD case was the 5-kNN using 7 features and achieving a value of 0.9323. Finally, a highest accuracy of 0.8887 was reached with Parzen in the DRT category using 42 features.

Table 1: Best accuracy obtained by each tested classifier and their corresponding optimal feature sets for each ME category.

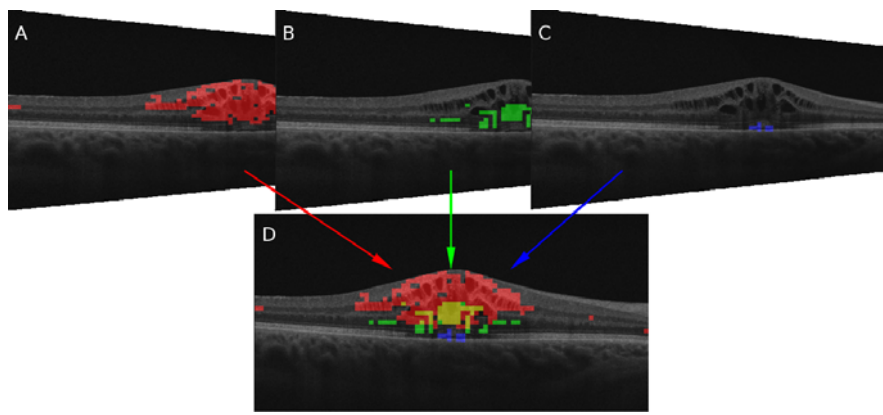|	*Category*	*LDC*	*3-kNN*	*5-kNN*	*7-kNN*	*Parzen*
CME	*N. Features*	42	19	19	21	19
	Accuracy	**0.9049**	0.8851	0.8846	0.8861	0.8872
SRD	*N. Features*	48	7	7	7	7
	Accuracy	0.8999	0.9295	**0.9323**	0.9285	0.9283
DRT	*N. Features*	5	34	8	8	42
	Accuracy	0.8701	0.8831	0.8804	0.8803	**0.8887**

Fig. 2: Partial binary identifications and merged color map. CME, DRT and SRD are represented as red, green and blue.

As explained, to facilitate the clinical diagnosis, a binary map is created for the identification of each type of ME. At the end, the 3 maps are merged into 1 unified color map that contains the 3 identifications, each one represented by a channel in the RGB space. This expresses, in an intuitive way, the presence of ME, helping the clinical experts in the analysis and diagnostic process, as the current method consists of a tedious and exhaustive manual review of the OCT images. As reference, Figure 2 shows the partial binary identifications and the merged color map that represents the 3 types of ME.

4   Conclusions

The ME analysis is of high relevance given it represents the 3rd main cause of blindness in developed countries. At the moment, its analysis and diagnosis involves a tedious and manual process of visual inspection to identify and characterize each ME type, which also carries the expert subjectivity.

In this work, a novel method is proposed for the automatic identification of the 3 ME categories using OCT images, following the international clinical classification of reference. To achieve this, we perform the identifications us-

ing a regional analysis that overcome the limitations of classical identifications, segmentations and FP removal in the issue. In order to do this, different classifiers were trained for each one of the categories to identify them separately. Finally, individual binary maps and a color map are created using the partial identifications, which facilitates the posterior clinical analysis and diagnosis. The proposed methodology was tested with 96 OCT images including the 3 ME categories, obtaining satisfactory results for the identification of each one.

References

[1] WHO. Vision impairment and blindness. *World Health Organization*, 2017.

[2] G. Trichonas and P. Kaiser. Optical coherence tomography imaging of macular oedema. *British Journal of Ophthalmology*, 98(Suppl 2):ii24–ii29, 2014.

[3] T. Otani, S. Kishi, and Y. Maruyama. Patterns of diabetic macular edema with optical coherence tomography. *American Journal of Ophthal.*, 127(6):688–693, 1999.

[4] G. Panozzo, B. Parolini, E. Gusson, A. Mercanti, S. Pinackatt, G. Bertoldo, and S. Pignatto. Diabetic macular edema: an OCT-based classification. *Seminars in Ophthalmology*, 19(1-2):13–20, 2004.

[5] Gary R Wilkins, Odette M Houghton, and Amy L Oldenburg. Automated segmentation of intraretinal cystoid fluid in optical coherence tomography. *IEEE Transactions on Biomedical Engineering*, 59(4):1109–1114, 2012.

[6] J. de Moura, J. Novo, J. Rouco, M. Penedo, and M. Ortega. Automatic Identification of Intraretinal Cystoid Regions in Optical Coherence Tomography. In *Conference on Artificial Intelligence in Medicine in Europe*, pages 305–315, 2017.

[7] J. de Moura, J. Novo, J. Rouco, and M. Ortega. Feature definition, analysis and selection for cystoid region characterization in Optical Coherence Tomography. *Procedia Computer Science*, 112:1369–1377, 2017.

[8] D. Sidibe, S. Sankar, G. Lemaitre, M. Rastgoo, J. Massich, C. Cheung, G. Tan, D. Milea, E. Lamoureux, and T. Wong. An anomaly detection approach for the identification of DME patients using spectral domain optical coherence tomography images. *Computer Methods and Programs in Biomedicine*, 139:109–117, 2017.

[9] A. Montuoro, S. Waldstein, B. Gerendas, U. Schmidt-Erfurth, and H. Bogunović. Joint retinal layer and fluid segmentation in OCT scans of eyes with severe macular edema using unsupervised representation and auto-context. *Biomedical Optics Express*, 8(3):1874–1888, 2017.

[10] K. Alsaih, G. Lemaitre, M. Rastgoo, J. Massich, D. Sidibé, and F. Meriaudeau. Machine learning techniques for diabetic macular edema (DME) classification on SD-OCT images. *Biomedical Engineering Online*, 16(1):68, 2017.

[11] G. Samagaio, J. de Moura, J. Novo, and M Ortega. Optical Coherence Tomography denoising by means of a fourier butterworth filter-based approach. In *International Conference on Image Analysis and Processing*, pages 422–432. Springer, 2017.

[12] S. Chiu, X. Li, P. Nicholas, C. Toth, J. Izatt, and S. Farsiu. Automatic segmentation of seven retinal layers in SDOCT images congruent with expert manual segmentation. *Optics Express*, 18(18):19413–19428, 2010.

[13] Plácido L Vidal, Joaquim de Moura, Jorge Novo, Manuel G Penedo, and Marcos Ortega. Intraretinal fluid identification via enhanced maps using optical coherence tomography images. *Biomedical Optics Express*, 9(10):4730–4754, 2018.